JOURNAL OF SOLID STATE CHEMISTRY 103, 481–489 (1993)

Topotactic Lithium Exchange in the Precursor Catalyst $VOHPO_4 \cdot 0.5H_2O$: The Crystal Structure of $LiVOPO_4 \cdot 0.5H_2O$

DIEGO LOZANO-CALERO, SEBASTIAN BRUQUE, MIGUEL A. G. ARANDA, MARIA MARTINEZ-LARA, AND LAUREANO MORENO

Departamento de Química Inorgánica, Universidad de Málaga, 29071 Malaga, Spain

Received March 30, 1992; in revised form September 25, 1992; accepted September 29, 1992

The synthesis and properties of a new lithium vanadyl(IV) phosphate, $LiVOPO_4 \cdot 0.5H_2O$, are reported. The synthesis was carried out by a lithium exchange reaction in $VO(HPO_4) \cdot 0.5H_2O$ with LiOH at low temperature in a nonaqueous medium. The crystal structure of $LiVOPO_4 \cdot 0.5H_2O$ (space group $P_{2_12_12_1}$, $a = 7.4651(6)$ Å, $b = 9.4167(8)$ Å, $c = 6.0762(6)$ Å, $Z = 4$) was refined by the Rietveld method from laboratory X-ray powder diffraction data, giving $R_{wp} = 8.0\%$ and $R_F = 6.5\%$. The structure is made up of layers made of VO_6 dimers which are linked by phosphate groups. The framework of the starting material is maintained but the vanadium coordination sphere is more distorted and the lithium position is deduced from a difference Fourier map. The structural, thermal, and spectroscopic features are compared to those of the closely related H-derivative.

Introduction

Intercalation systems have recently become of great interest due to the different materials that can be synthesized with applicability as batteries, sensors, or catalysts (*1*). Among these compounds, the phosphates and arsenates of vanadium and niobium oxocations constitute an important series and have been the subject of considerable attention due to their rich chemistry (*2–4*). The synthetic efforts have been directed toward the exchange or insertion of metal cations into the channels or between the layers of these phosphates. Lithium is one of the most used for these purposes because of its small size, which allows it to be accommodated easily into the host network. The solids obtained in this way have been studied to determine the metal cations' environments and the role they play in affecting the host framework. Several lithium derivatives of phosphates and arsenates of vanadyl or niobyl have recently been reported. Interest in these systems is due to the changes in the electronic and structural properties and their potential applications, for example as ionic conductors. Thus, some of these materials exhibit high ionic conductivity as $(LiOH)_xNbOPO_4$ ($x = 0.25$, 0.5, 1.0, 1.5) (*5*) and $Li_{1.6}(V_{0.6}^{IV}V_{0.4}^{V}O)PO_4(OH)$ (*6*). Jacobson *et al.* (*7*) claimed that the solid $LiVOPO_4 \cdot 2H_2O$ is a tetragonal phase derived from $VOPO_4 \cdot 2H_2O$. Lavrov *et al.* (*8*) and Lii *et al.* (*9*) have described the structures of α-$LiVOPO_4$ and β-$LiVOPO_4$, showing that they belong to the triclinic and orthorhombic

0022-4596/93 $5.00

crystallographic systems, respectively. $Li_4VO(AsO_4)_2$ has been synthesized by lithium exchange of $VO(H_2AsO_4)_2$ at low temperature (*10*) and its structure has been determined using powder X-ray diffraction data (*11*). The frameworks of these solids remain unaltered, this case being a clear example of topotactic transformation.

A great attention has been paid to the vanadyl(IV) hydrogen phosphates during recent years and especially to $VO(HPO_4) \cdot 0.5H_2O$ (*12–14*), which is the precursor of the active catalytic phase in the production of maleic anhydride from butane and air (*13*). In a structural study from single crystal X-ray diffraction data, $VO(HPO_4) \cdot 0.5H_2O$ was shown to have a layer structure (*14*). The accessibility of its interlamellar space for cations by "chimie douce" and the effects of this incorporation are two very interesting topics for research. In this paper we describe the lithium exchange reaction in $VO(HPO_4) \cdot 0.5H_2O$, the crystal structure, and the thermal and spectroscopic characterization of a new Li-derivative, $LiVOPO_4 \cdot 0.5H_2O$.

Experimental

$VO(HPO_4) \cdot 0.5H_2O$ was synthesized following the method proposed by Johnson *et al.* (*13*), who made the reduction of V_2O_5 with i-ButOH in the presence of H_3PO_4. $LiVOPO_4 \cdot 0.5H_2O$ was prepared by stirring a suspension of 0.5 g of $VO(HPO_4) \cdot 0.5H_2O$ and 0.24 g of $LiOH \cdot H_2O$ (Aldrich, 99.95%) in 20 ml of methanol for 3 weeks at room temperature. The mixture was put into a sealed tube to avoid contamination with CO_2 from the air. The blue-greenish suspension was filtered off, and the solid was washed twice with 20 ml of methanol which contained two drops of concentrated hydrochloric acid, and finally with another 20 ml of methanol. It was stored in a dry atmosphere.

The lithium exchange cannot be carried out in an aqueous medium because $VO(HPO_4) \cdot 0.5H_2O$ and $LiVOPO_4 \cdot 0.5H_2O$ are soluble in water. Therefore, less polar media such as acetone, ethanol, or methanol must be used.

We tried to obtain the lithium derivative from direct synthesis, following the same method that leads to the H-derivative [$VO(HPO_4) \cdot 0.5H_2O$]. Thus, $V_2O_5/H_3PO_4/LiOH$ were mixed and refluxed for 72 hr in isobutanol, but a very complex mixture of nonidentified phases was obtained.

The chemical analysis were carried out by dissolving the solids in dilute H_2SO_4. The vanadium content was measured by atomic absorption spectrophotometry and the lithium content by flame emission spectrophotometry, whereas phosphorus was determined by colorimetry as the blue molybdophosphate complex. Water content was determined thermogravimetrically. The stoichiometry has been proposed on the basis of analytical results. Calculated for $LiVOPO_4 \cdot 0.5H_2O$: Li, 3.9%; V, 28.7%; P, 17.4%; H_2O, 5.2%. Found: Li, 3.8%; V, 28.9%; P, 17.5%; H_2O, 5.0%. Calculated for $VO(HPO_4) \cdot 0.5H_2O$: V, 29.7%; P, 18.0%; H_2O, 10.4%. Found: V, 29.6%; P, 17.9%; H_2O, 9.1%.

Thermal analysis (TGA and DTA) was carried out in air on a Rigaku Termoflex apparatus at a heating rate of 10°C min^{-1} with calcinated Al_2O_3 as the reference. Infrared spectra were recorded on a Perkin–Elmer 883 spectrometer using a dry KBr pellet containing 2% of the sample. The diffuse reflectance spectra (UV–vis–near IR) were obtained on a Shimadzu UV-3100 spectrophotometer equipped with an integrating sphere and using $BaSO_4$ as the reference blank. X-ray powder diffraction patterns were obtained with a Siemens D-501 automated diffractometer using graphite-monochromated Cu$K\alpha$ radiation. The powder pattern for $LiVOPO_4 \cdot 0.5H_2O$ was recorded in 0.03° [2θ] steps between 13° and 75° [2θ] counting for 13 sec per point, and

was transferred to a VAX 8530 computer for analysis. Rietveld refinements (*15*) were performed with GSAS program (*16*) using a pseudo-Voigt peak shape function, corrected for asymmetry at low angles. The scanning electron micrographs were made using a JEOL S.M. 840 device to observe the morphology and particle size of the solids.

Results and Discussion

The scanning electron photomicrographs (see Fig. 1) show that the original plate-like morphology is retained but the size of individual microparticles is smaller (less than 1 μm), the distribution of size is not homogeneous, and finally, the edge of the microparticles presents an irregular profile, which may be associated to a minor amorphous or low-crystalline phase.

The powder pattern of the lithium vanadyl(IV) phosphate hemihydrate was indexed with the TREOR program (*17*) on an orthorhombic unit cell with a = 7.444(2) Å, b =9.394(0) Å and c= 6.057(5) Å, and figures of merit M_{20} = 39 (*18*) and F_{20} = 46 (0.009, 52) (*19*). This unit cell is similar to that of the parent compound, $VO(HPO_4) \cdot 0.5H_2O$, a = 7.420(1) Å, b = 9.609(2) Å, and c = 5.693(1) Å. The a and b parameters do not change greatly, but the c parameter increases about 0.4 Å to accommodate the metal cations.

The systematic absences of odd $h00$ and odd $0k0$ reflections and the presence of $hk0$ reflections with odd $h + k$ in the powder pattern reveal that the symmetry has fallen from *Pmmm* (space group of the $VO(HPO_4) \cdot 0.5H_2O$) to its maximal nonisomorphic subgroup $P_{2_12_12}$. Hence, the crystal structure of $LiVOPO_4 \cdot 0.5H_2O$ was refined by the Rietveld method using the coordinates of $VO(HPO_4) \cdot 0.5H_2O$ (*14*) as starting model, but lowering the space group symmetry. Lithium atom position was assigned constructing a Fourier difference map. In the final refinement, all the atomic coordinates were refined independently; only an isotropic temperature factor was varied due to the limited data range used and converged to B_{ISO} = 0.71(6), giving R_{wp} = 8.0% and R_F = 6.5%. On the other hand, as result of the presence of an amorphous phase and impurities (we estimate <5% from the X-ray diffracton data), the background had an irregular variation, being fitted manually. Results are given in Table I, and the final observed, calculated and difference profiles are displayed in Fig. 2. The impurities cause very weak peaks near 22°, 34°, and 37°(2θ) whose intensities depend on the time reaction. Final bond distances and angles are given in Table II. A polyhedral Struplo (*20*) representation of the framework of $LiVOPO_4 \cdot 0.5H_2O$ and $VO(HPO_4) \cdot 0.5H_2O$ is shown in Figs. 3 and 4.

The crystal structure of $LiVOPO_4 \cdot 0.5H_2O$ (Fig. 3) consists of vanadyl phosphate layers stacked along the c axis and held together by interlayer lithium ions. The layers contain dimers of face-sharing VO_6 units and are linked among them by phosphate groups. The VO_6 units are distorted octahedra which contain four unequal equatorial distances V–O and one short apical distance corresponding to V=O(4) and a larger distance corresponding to $V–OH_2$ (O(w), in Table II). The water molecule is located at the apical vertex bridging two VO_6 units. Three oxygens of PO_4 are shared with three different vanadium atoms, and the fourth (O(1), see Table II) is charged negatively and is directed towards the interlamellar space, which allows it to hold the layers together electrostatically by interaction with the lithium atoms. As one could expect, the lithium cations are situated near these oxygens attracted by their negative charge (see Fig. 3) and are located in an irregular, five-coordinate site, with Li–O distances varying between 1.91 and 2.67 Å.

The framework of $LiVOPO_4 \cdot 0.5H_2O$ is basically equal to the $VO(HPO_4) \cdot 0.5H_2O$

FIG. 1. SEM micrographs of (a) $VO(HPO_4) \cdot 0.5H_2O$, (b) $LiVOPO_4 \cdot 0.5H_2O$.

(Fig. 4). The more prominent differences between them are that the lithium derivative presents a larger distortion in the VO_6 units and PO_4 groups and the disappearance of the P–OH.

Thermogravimetric analysis of the two solids, starting $VO(HPO_4) \cdot 0.5H_2O$ and lithium derivative $LiVOPO_4 \cdot 0.5H_2O$, shows substantial differences between them. The TGA–DTA curves for these compounds are

TABLE I

CRYSTALLOGRAPHIC AND STRUCTURAL PARAMETERS FOR $LiVOPO_4 \cdot 0.5H_2O$ (SPACE GROUP $P_{2_12_12}$ (No. 18))

Unit cell parameters

a = 7.4651(6) Å b = 9.4167(8) Å c = 6.0762(6) Å
V = 427.14(5) Å^3 Z = 4

No. of allowed reflections = 312 No. of variables = 36
No. of points in refinement = 2067

R Factors (%)

R_F = 6.5 R_{wp} = 8.0 R_p = 6.0

Atomic Parameters

Atom	Sym. pos.	x	y	z
V	4c	−0.2031(5)	−0.002(1)	−0.0056(7)
P	4c	0.009(2)	0.2672(7)	0.21911(9)
O(1)	4c	−0.028(3)	0.212(1)	0.457(1)
O(2a)	4c	−0.159(3)	0.353(2)	0.164(4)
O(2b)	4c	0.184(3)	0.355(2)	0.181(4)
O(3)	4c	−0.013(4)	0.1494(9)	0.046(2)
O(4)	4c	−0.296(1)	0.033(2)	0.233(2)
O(w)	2a	0	0	−0.292(3)
Li	4c	0.214(7)	0.166(4)	0.529(9)

TABLE II

SELECTED BOND DISTANCES (Å) AND ANGLES (°) FOR $LiVOPO_4 \cdot 0.5H_2O$

V–O(2a)	1.96(2)	Li–O(1)	1.91(6)
V–O(2b)	1.937(2)	Li–O(1)	2.24(5)
V–O(3)	2.04(2)	Li–O(2a)	2.10(5)
V–O(3)	2.15(2)	Li–O(4)	2.67(5)
V–O(4)	1.64(1)	Li–O(w)	2.48(4)
V–O(w)	2.31(1)		
P–O(1)	1.566(8)		
P–O(2a)	1.537(8)		
P–O(2b)	1.558(8)		
P–O(3)	1.536(7)		
O(2a)–V–O(2b)	89.8(5)	O(1)–P–O(2a)	103.1(2)
O(2a)–V–O(3)	158.3(8)	O(1)–P–O(2b)	117.7(2)
O(2a)–V–O(3)	91.1(1)	O(1)–P–O(3)	111.8(8)
O(2a)–V–O(4)	110.8(1)	O(3)–P–O(2a)	98.1(1)
O(2b)–V–O(3)	83.7(1)	O(2b)–P–O(3)	112.2(2)
O(2b)–V–O(3)	150.1(8)	O(2a)–P–O(2b)	111.8(8)
O(2b)–V–O(4)	99.0(1)	V–O(2a)–P	154.7(2)
O(3)–V–O(3)	84.6(5)	V–O(2b)–P	145.5(2)
O(3)–V–O(4)	90.7(8)	V–O(3)–V	92.8(4)
O(3)–V–O(4)	108.5(6)	V–O(3)–P	133.8(2)
		V–O(3)–P	118.8(2)

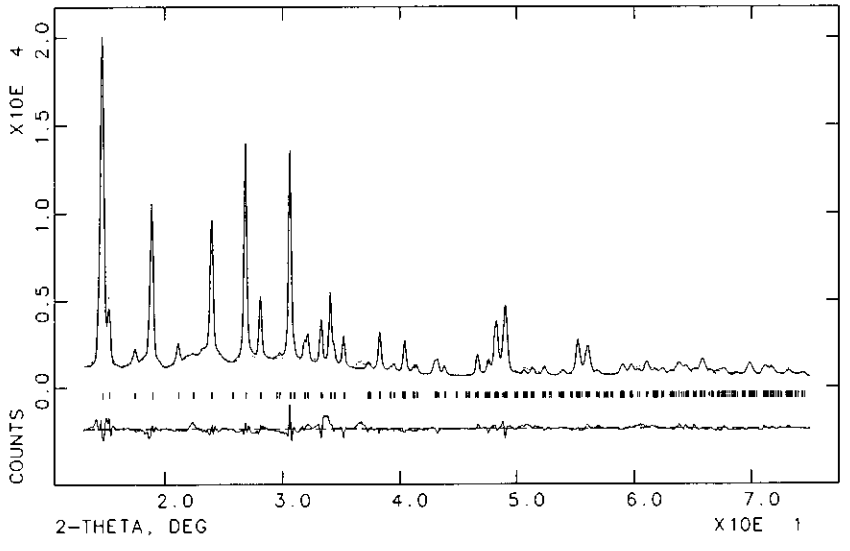

FIG. 2. Final (observed) points, calculated (full line), and difference X-ray profiles for $LiVOPO_4 \cdot 0.5H_2O$.

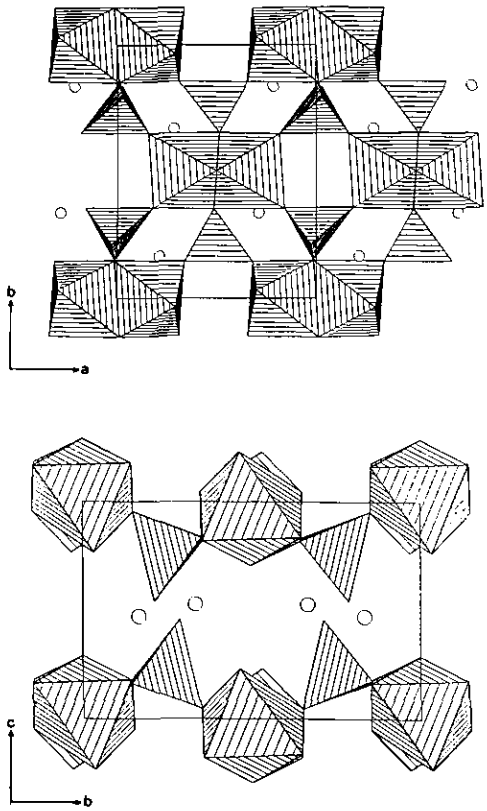

FIG. 3. Polyhedral views of $LiVOPO_4 \cdot 0.5H_2O$: (a) along the c axis and (b) along the a axis.

shown in Fig. 5. $LiVOPO_4 \cdot 0.5H_2O$ shows curves completely distinct from its parent compound. The TG curve decreases continuously and loss of water begins at 60°C and ends near 250°C, having two diffuse endotherms near 65 and 130°C. This lower temperature required to dehydrate can be explained because the water is not so strongly bonded as in the precursor, $VO(HPO_4) \cdot 0.5H_2O$, and because the structure is more open after the lithium exchange. The substitution of the protons by Li^+ has been very efficient and does not remain HPO_4^{2-} groups after insertion because no sort of hydrogenphosphate to pyrophosphate condensation can be observed when $LiVOPO_4 \cdot 0.5H_2O$ is heated. The exothermic and endothermic effects without loss weight centered at 330, 392, and 407°C and 560 and 600°C respectively can be observed. A thermodiffractometric study was carried out to detect the transformations which take place at 250, 400, and 600°C. The X-ray powder patterns of the heating products can be seen in Fig. 6. This study reveals the existence of a destructive transformation when the water is lost, but a new phase starts forming at 400°C and becomes a crystalline single phase at 600°C, which can be indexed in the orthorhombic system (a= 10.303(3), b = 8.545(2), c= 4.625(1), M_{20} = 34). This phase was found by Pozas *et al.*(6) in a system Li–V–P–O.

These kinds of phase transformations are typical in lithium derivatives of these phos-

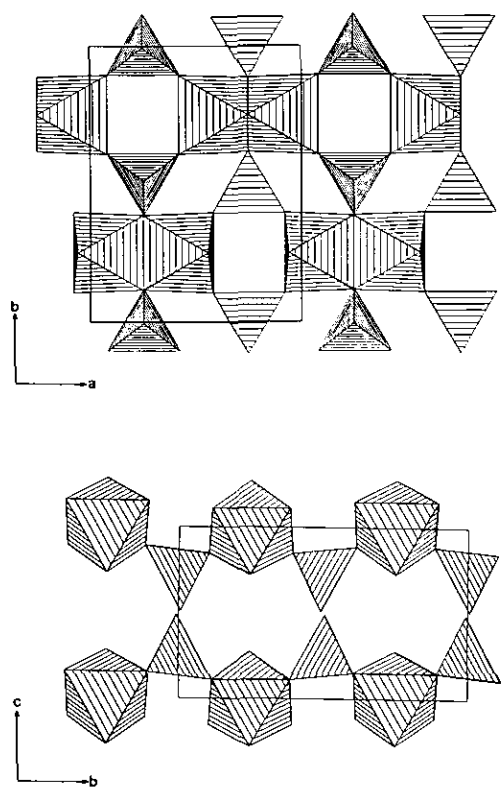

FIG. 4. Polyhedral views of $VO(HPO_4) \cdot 0.5H_2O$: (a) along the c axis and (b) along the a axis.

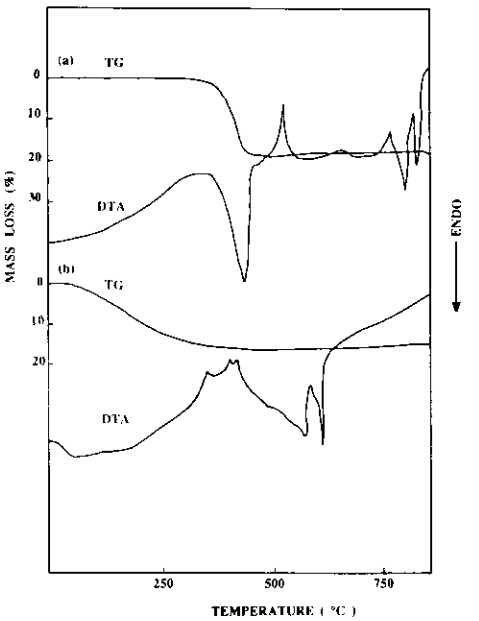

FIG. 5. Thermal analysis (TGA and DTA) of (a) $VO(HPO_4) \cdot 0.5H_2O$, (b) $LiVOPO_4 \cdot 0.5H_2O$.

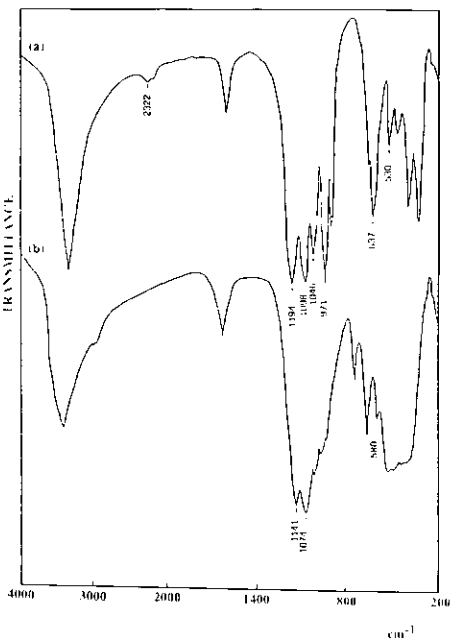

FIG. 7. Infrared spectra of (a) $VO(HPO_4) \cdot 0.5H_2O$, (b) $LiVOPO_4 \cdot 0.5H_2O$.

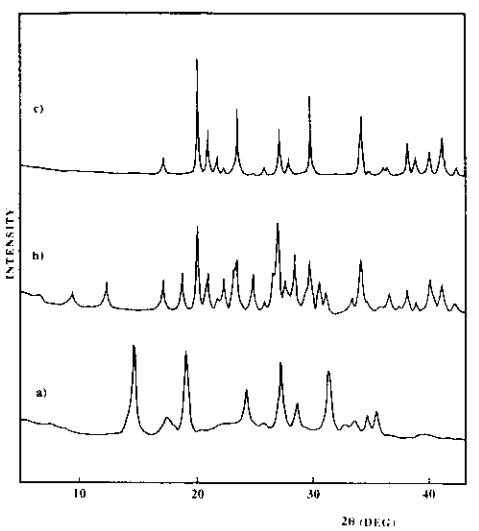

FIG. 6. X-ray powder patterns of resulting products when $LiVOPO_4 \cdot 0.5H_2O$ is heated at (a) 250°C, (b) 400°C, and (c) 600°C (orthorhombic phase, see text).

phates (*5*), probably due to the migration of the Li^+ cations to more thermodynamically stable sites.

The IR spectrum of the $LiVOPO_4 \cdot 0.5H_2O$, together with that of the parent compound $VO(HPO_4) \cdot 0.5H_2O$, can be seen in Fig. 7. The comparison of the two spectra reveals, as main feature, that the bands at 2322 cm^{-1} (stretching POH), 1194 cm^{-1} (bending POH), and 637 cm^{-1} (out-of-plane bending POH) (*21–23*) disappear in $LiVOPO_4 \cdot 0.5H_2O$. Strong absorption bands are observed in the 900–1200 cm^{-1} range which are characteristic of orthophosphate solids. More vibration modes become active because the PO_4 local symmetry is distorted and falls to C_1, and therefore a splitting of the υ_3 vibration appears. Thus the bands appearing at 1141 cm^{-1} and 1074 cm^{-1} can be assigned as $\upsilon_{asym.}$ and $\upsilon_{sym.}$ stretching, respectively, in the lithium vanadyl(IV) phosphate and to ones at 1098 cm^{-1} and 1046

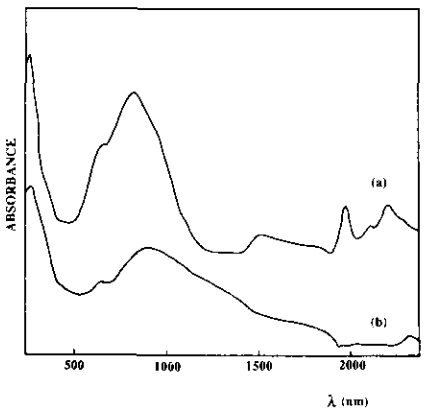

FIG. 8. Diffuse reflectance spectra of (a) $VO(HPO_4) \cdot 0.5H_2O$, (b) $LiVOPO_4 \cdot 0.5H_2O$.

cm^{-1}, respectively, in the vanadyl hydrogenphosphate. The band centered at 530 cm^{-1} in $VO(HPO_4) \cdot 0.5H_2O$, which is assigned to the asymmetric deformation $\delta_{as(OPO)}$, is affected and shifts to a higher frequency (580 cm^{-1}) in $LiVOPO_4 \cdot 0.5H_2O$ due to the PO_4 unit being more distorted. The presence of VO^{2+} moieties is seen by the characteristic absorption at 971 cm^{-1} that corresponds to the V^{IV}=O stretching vibration and it agrees with other reports for related compounds (*11, 25, 26*). The position of this band does not change in the lithium exchange reaction, showing that the oxidation state of the vanadium atom has remained (V^{V}=O stretching vibration absorbs at higher frequency, 1000 cm^{-1}). Finally the bands associated with the water are clearly distinguished (3382 cm^{-1}, stretching, and 1630 cm^{-1}, bending).

The diffuse reflectance spectra of $VO(HPO_4) \cdot 0.5H_2O$ and $LiVOPO_4 \cdot 0.5H_2O$ are shown in Fig. 8. The profile of both spectra are the same in the UV–Vis region and consists of a set of three bands and a shoulder. Similar spectra have been reported in the literature for related systems (*11, 23*).

The higher symmetry that could be expected for an oxovanadium(IV) would be C_{4v} and in this case there would be three potential intra-*d*-shell electronic transitions (I: $e^* \leftarrow b_2$, II: $b_1 \leftarrow b_2$, III: $1a_1 \leftarrow b_2$). Probably the first two transitions overlap, and lie under a unique band but when the symmetry decreases, the degenerancy of the *e* level will be lifted so that all the transitions would be potentially observable (*27*). Taking into account these features and knowing that the vanadium atoms in $LiVOPO_4 \cdot 0.5H_2O$ and $VO(HPO_4) \cdot 0.5H_2O$ have a pseudo-C_{2v} and pseudo-C_{4v} symmetry respectively, the bands have been assigned as seen in Table III. The two absorption bands near to 260 nm are too strong and energetic to be *d–d* transition, and fall into the ultraviolet region. They are assigned as oxygen to vanadium charge transfer bands. Furthermore, they overlap the $^2A_1 \leftarrow {}^2B_2$ electronic transit that appears like a shoulder.

There are more differences in the near-infrared region, which comprises four bands for $VO(HPO_4) \cdot 0.5H_2O$, whereas no such bands as those can be observed in $LiVOPO_4 \cdot 0.5H_2O$. The wide band centered at 1550 nm can be assigned to a υ_{HOH} overtone and a combination one of υ_{HOH} and δ_{HOH} appears at 2220 nm.

TABLE III

DIFFUSE REFLECTANCE DATA FOR $VO(HPO_4) \cdot 0.5H_2O$ AND $LiVOPO_4 \cdot 0.5H_2O$

Value (nm)	Value (cm^{-1})	Assignment
	absorption	
	$VO(HPO_4) \cdot 0.5H_2O$	
265	37730	charge transfer
≈325	≈30770	$^2A_1 \leftarrow {}^2B_2$
656	15240	$^2B_1 \leftarrow {}^2B_2$
829	12120	$^2E \leftarrow {}^2B_2$
1550	6450	2υ(OH)
2220	4500	υ(OH) + δ(HOH)
	absorption	
	$LiVOPO_4 \cdot 0.5H_2O$	
264	37730	charge transfer
—	—	$^2A_1 \leftarrow {}^2B_2$
645	15500	$^2B_1 \leftarrow {}^2B_2$
901	11100	$^2E \leftarrow {}^2B_2$

Conclusions

A novel lithium vanadyl(IV) phosphate has been synthesized by H^+/Li^+ exchange at low temperature. The substitution of the protons causes only a slight effect on the original lattice of the $VO(HPO_4) \cdot 0.5H_2O$; therefore this exchange reaction can be regarded as topotactic because no bonds have been broken in the framework. The new compound is metastable and structurally sensitive to the dehydration and the heating. The environment of Li^+ cations is irregular and its geometry is inadequate for fast ion transport. At temperatures higher than 600°C the $LiVOPO_4 \cdot 0.5H_2O$ forms a single orthorhombic phase.

The coordination geometry around both vanadium and phosphorus atoms is similar in $VO(HPO_4) \cdot 0.5H_2O$ and $LiVOPO_4 \cdot 0.5H_2O$ compounds, although the vanadium coordination sphere in the lithium derivative is more distorted. The diffuse reflectance spectrum of this compound agrees well to this less regular environment.

We have shown that the Rietveld method, using X-ray laboratory powder diffraction data, is a very useful and cheap tool for deriving structural information, especially after an ionic exchange reaction, when single crystals cannot be synthesized and the final compound is sufficiently crystalline.

Acknowledgments

D.L.C. and M.G.A. thank the Ministerio de Educación y Ciencia (Spain) for the provision studentship.

References

1. D. W. Murphy, S. A. Sushire, and S. M. Zahurak, *in* "Chemical Physics of Intercalation," NATO ASI Series, Series B: Physics, Vol. 172, p. 173, Plenum, New York (1987).
2. M. Martinez-Lara, L. Moreno-Real, A. Jimenez-Lopez, S. Bruque, B. Casal, and E. Ruiz-Hitzky, *Mater. Res. Bull.* **20,** 49 (1988).
3. M. Martinez-Lara, L. Moreno-Real, A. Jimenez-Lopez, S. Bruque, and E. Rodriguez-Garcia, *Mater. Res. Bull.* **21,** 13 (1986).
4. G. Ladwig, *Z. Anorg. Allg. Chem.* **338,** 266 (1965).
5. L. Moreno-Real, T. Ramirez-Cardenas, S. Bruque, M. Martinez-Lara, and J. R. Ramos-Barrado, *Mater. Res. Soc. Sympos. Proc.* **210,** 687 (1991).
6. R. Pozas, S. Madueño, S. Bruque, L. Moreno-Real, M. Martinez-Lara, C. Criado, and J. R. Ramos-Barrado, *Solid State Ionics* **51,** 79 (1992).
7. A. J. Jacobson, J. W. Johnson, J. F. Brody, J. C. Scanlon, and J. K. Lewandowski, *Inorg. Chem.* **24,** 1782 (1985).
8. A. V. Lavrov, V. P. Nikolaev, G. G. Sadikov, and M. A. Porai-Koshits, *Sov. Phys. Dokl.* **27,** 680 (1987).
9. K. H. Lii, C. H. Li, C. Y. Cheng, and S. L. Wang, *J. Solid State Chem.* **95,** 352 (1991).
10. M. Martinez-Lara, S. Bruque, L. Moreno-Real, and M. A. G. Aranda, *J. Solid State Chem.* **91,** 25 (1991).
11. M. A. G. Aranda, P. J. Attfield, S. Bruque, and M. Martinez-Lara, *Inorg. Chem.* **31,** 1045 (1992).
12. C. C. Torardi and J. C. Calabrese, *Inorg. Chem.* **23,** 1308 (1984).
13. J. W. Johnson, D. C. Johnston, A. J. Jacobson, and J. F. Brody, *J. Am. Chem. Soc.* **106,** 8123 (1984).
14. M. E. Leonowicz, J. W. Johnson, J. F. Brody, H. F. Shannon, Jr., and J. M. Newsam, *J. Solid State Chem.* **56,** 370 (1985).
15. H. M. Rietveld, *J. Appl. Crystallogr.* **2,** 65 (1969).
16. A. C. Larson and R. B. von Dreele, "Los Alamos National Laboratory Report No. LA-UR-86-748" (1987).
17. P. E. Werner, *Z. Kristallogr.* **120,** 375 (1969).
18. P. M. de Wolf, *J. Appl. Crystallogr.* **1,** 108 (1968).
19. G. S. Smith and R. L. Snyder, *J. Appl. Crystallogr.* **12,** 60 (1979).
20. R. X. Fischer, *J. Appl. Crystallogr.* **18,** 258 (1985).
21. N. Casañ, P. Amoros, R. Ibañez, E. Martinez-Tamayo, and D. Beltran-Porter, *J. Inclusion Phenomena* **6,** 193 (1988).
22. L. V. Kobets, and D. S. Umreiko, *Russ. Chem. Rev.* **52,** 6 (1986).
23. P. Amoros, R. Ibañez, E. Martinez-Tamayo, A. Beltran-Porter, and D. Beltran-Porter, *Mater. Res. Bull.* **24,** 1347 (1989).
24. K. Nakamoto, *in* "Infrared Spectra of Inorganic and Coordination Compounds," 4th ed., Wiley, New York (1986).
25. J. E. Baran and B. S. Etcheverry, *Polyhedron* **4**(10), 1711 (1985).
26. G. Busca, F. Cavani, G. Centi, and F. Trifiro, *J. Catal.* **99,** 400 (1986).
27. A. B. P. Lever, *in* "Inorganic Electronic Spectroscopy," 2nd ed., Elsevier, Amsterdam (1984).